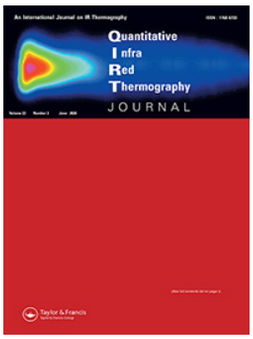

Quantitative InfraRed Thermography Journal

ISSN: 1768-6733 (Print) 2116-7176 (Online) Journal homepage: www.tandfonline.com/journals/tqrt20

Quantitative evaluation of the rate of thermal response in the lower extremities on individuals with and without type 2 diabetes mellitus

Rosalinda Ortiz-Sosa, Edgar I. Fuentes-Oliver , Raúl Serrano-Loyola , Rebeca Solalinde-Vargas & Crescencio García-Segundo

To cite this article: Rosalinda Ortiz-Sosa, Edgar I. Fuentes-Oliver , Raúl Serrano-Loyola , Rebeca Solalinde-Vargas & Crescencio García-Segundo (28 May 2026): Quantitative evaluation of the rate of thermal response in the lower extremities on individuals with and without type 2 diabetes mellitus, Quantitative InfraRed Thermography Journal, DOI: 10.1080/17686733.2026.2676638

To link to this article: https://doi.org/10.1080/17686733.2026.2676638

Published online: 28 May 2026.

QUANTITATIVE INFRARED THERMOGRAPHY JOURNAL
https://doi.org/10.1080/17686733.2026.2676638

Quantitative evaluation of the rate of thermal response in the lower extremities on individuals with and without type 2 diabetes mellitus

Rosalinda Ortiz-Sosa[a,b], Edgar I. Fuentes-Oliver[a,b], Raúl Serrano-Loyola[c], Rebeca Solalinde-Vargas[c] and Crescencio García-Segundo[a,d]

[a]ICAT, Universidad Nacional Autónoma de México, Mexico City, Mexico; [b]Facultad de Ciencias, Universidad Nacional Autónoma de México, Mexico City, Mexico; [c]Servicio de Radiología Intervencionista, Hospital General de México, Mexico City, Mexico; [d]Sabbatical Leave at Institute of Biological and Medical Imaging, Helmholtz Zentrum, München, Germany

ABSTRACT

A quantifier of the thermal response to a thermal challenge in the lower extremities can reveal peripheral impairment in patients with type 2 Diabetes Mellitus (DM2), aiding timely diagnosis and treatment. This study introduces the parameter V_{ri} as a feasible quantifier of metabolic performance in a temperature regulation process of the lower limbs of individuals with DM2. This index is derived from the analysis of an infrared image sequence through the rate of recovery of metabolic heat of the lower limbs after an instantaneous thermal stimulus, termed the *slope value index*. The same thermal challenge is applied to a group of patients with DM2 and control volunteers, also clinically supervised. Evaluation of V_{ri} showed reduced recovery performance in patients with DM2 compared to the performance exhibited by the control group. According to ROC analysis, this parameter V_{ri} yielded sensitivity and specificity above 0.8, reaching 92% and 83%, respectively. An additional result is that distance $\bar{V}_{ri}$ shows that its correlation with clinical variables is statistically significant: glucose ($p < 0.01$) and HbA1c ($p < 0.001$). This method offers a non-radiative and non-invasive approach for assessing metabolic deterioration in the lower extremities, potentially suitable for unlimited use both in diagnosis and during treatment.

ARTICLE HISTORY
Received 25 November 2025
Accepted 8 May 2026

KEYWORD
Thermal response; type 2 diabetes mellitus; diabetic foot disease; biomedical infrared imaging; temperature regulation

1. Introduction

Body temperature regulation is the result of several biological functions and a large number of physiological and neurological self-regulatory mechanisms; vasoconstriction, vasodilation, sweating, heat redistribution by convection through blood flow, and heat exchange with the environment, among others [1]. The simplified description of human temperature regulation is associated with the dissipation and radiation of excess metabolic heat, which is the result of biological, chemical and physical activity; that is, the work done as a result of the interaction of the body with the surroundings [2]. The metabolic heat network is supported by the vascular system, which acts as a regulation agent through the balanced or controlled action of the sympathetic and parasympathetic systems [3,4]. For this reason, this network follows distribution patterns determined by characteristics that in some way form a fingerprint of human anatomy and its related physiology [5].

Metabolic disorders such as long-term type 2 diabetes mellitus (DM2) often cause impairment of both the vascular system and heat regulation mechanisms, which means that the heat distribution network and, consequently, the associated thermal patterns also change. Interestingly, these alterations in the limbs occur at different rates, which promotes asymmetric alterations of the natural anatomical metabolic heat distribution [6,7]. This is the onset scheme for body damage, which can lead, in advanced stages, to deterioration of lower limb function, otherwise known as diabetic foot disease (DFD) [8,9].

To reduce the impact of complications related to type 2 diabetes mellitus, accessible tools are necessary that can contribute to the timely identification of peripheral nerve damage and vascular damage in the lower limbs. Hence, the use of infrared cameras to remotely visualise metabolic heat distribution has prompted

CONTACT Rosalinda Ortiz-Sosa rortizsosa@ciencias.unam.mx ICAT, Universidad Nacional Autónoma de México, Cto. Exterior S/N, C.U., Coyoacán, Mexico City 04510, Mexico

research in the field of biomedical infrared imaging (BMIRI) [10], and consequently, numerous studies have focused on proving and validating the use of this type of imaging as a tool to support clinical diagnosis. A significant part of this research is focused on the use of infrared thermography of the soles of the feet to assess the risk of diabetic foot ulceration [11–15]. This trend is also reflected in the bibliographic review presented in [16]. In contrast, other studies use infrared images of the legs to obtain information regarding peripheral damage and assess the likelihood of developing foot ulcers [4,6,17]. Detecting abnormalities directly in the leg improves the effectiveness of preventive screening.

One of the arising difficulties for IR imaging to reach the quantitative grade relates to the lack of strategies able to get reliable referencing or baseline standards, in view of the difficulties to validate the reproducibility and stability of the results. Thus, the corresponding number of reports is quite scarce, as can be verified through a thorough search in specialised data bases, such as Scopus [18–21]. There is a much broader list of contributions on BMIRI, covering in a comprehensive manner several types of studies, clinical, non-clinical and including wounds and other types of tissue damage. The interested reader can consult, for instance [22], which is an authoritative updated review. As highlighted above, one of the main objectives to reach the quantitative stage, is to get the validation of BMIRI, specific for the study of metabolic heat disorders caused by type 2 diabetes mellitus (DM2) and the development of tools to support the early clinical diagnosis of DFD, with an emphasis on the prevention of amputations in the general population [8,9].

The present report is part of the research programme whose previous results were published in the references [6,17,23], and the objective is to develop tools to support the early clinical diagnosis of peripheral damage caused by long-term DM2. The current novelty relies on the simple and direct graphical representation of the quantifiable metabolic performance of the basal state, when compared against its temporal response to a controlled external stimulus. That is applied equally to each participant. Such performance, in each participant, is characterised by the temporal change of the radiometric asymmetry; i.e. the time response to the external thermal stimulus, which, in turn, is an inherent characteristic of each individual. The noted representation appears here as the novel slope value index (SVI). This parameter provides not only a cross-sectional assessment of the limbs, but also a partially longitudinal assessment, which strengthens the information obtained from the infrared images acquired from each individual. The protocol required for acquiring the related information, requires a significantly different handling of the participants, including the inclusion–exclusion criteria, which is more stringent with respect to that protocol in previous reports. That also extends to the handling of the imaging processing and data extraction. Image stability and methodological reproducibility are also additional features that add to consistency and confidence displayed by the emerging results. The results presented here correspond to an examination of the response to a temperature regulation process in the lower extremities in subjects clinically diagnosed with DM2, when we analyse the short-term evolution of the thermal patterns distributed in the lower extremities, compared to the performance of control individuals, which have a negative diagnosis of this disease. For this purpose, infrared image sequences are obtained, under controlled and reproducible conditions, for studying the time response of the lower limb tissue of the participant individuals. The characteristic thermal patterns are altered through a partially controlled external thermal stimulus: a simultaneously gentle moist of the lower limbs. Clinical analysis shows that changes in the pattern distribution of metabolic heat, as well as the speed of change and recovery, are fairly different between healthy individuals, compared to those of patients free from the characteristic markers that define DFD. The results of this study suggest that by assessing the performance of the temperature regulation process, it is possible to visualise alterations in metabolic heat in the lower extremities as a consequence of the long-term evolution of DM2, prior to the appearance of characteristic lesions of the DFD.

1.1. Asymmetry and thermal response index

Various authors have highlighted the importance of obtaining relevant information through thermal patterns of the lower extremities to identify metabolic alterations due to the long-term evolution of type 2 diabetes mellitus. These alterations can be identified due to physiological characteristics such as thermal symmetry [6,12,24–26] or the behaviour of biological tissue under challenges of vasodilation or vasoconstriction [27–30].

Taking into account the above, our research group proposed a data analysis that involves a thermal response test, using the concept of thermal asymmetry and introducing the so-called Asymmetry and Thermal Response index (ATR-index) [7,17]. This index indicates the relationship between the measure of asymmetry between the contra lateral limbs and also the response they present to a thermal stimulus. By changing the moment of measurement of the asymmetry, the authors can evaluate not only the thermal performance of each individual in a transverse way but also partially longitudinally.

The design of the ATR index allows for a general assessment of the thermobiological performance in the lower extremities, considering both thermal asymmetry and the response of biological tissue to a challenge of vasodilation, triggered by the response of the sympathetic neural system. Since the results presented previously were based solely on the analysis of the symmetry of the baseline state, this study expands this assessment by studying the evolution of thermal performance over a period spanning from the time immediately following the application of the thermal stimulus until it reaches thermal stability. In other words, the application of the ATR-index is extended to examine the performance of the lower extremities in both patients and controls at different times during a thermal regulation process. This information represents the instantaneous and time-evolution response of each individual subject to the test. Since the method applies the same to the control and patient individuals, the expected outcome is to disclose a differentiated response between the patients and controls, having the metabolic alteration as the differentiation parameter.

The introduction of the ATR-index is obtained using the concept of cross-entropy as a measure of the distance between two probability distributions of a random variable. The index is described according to Equation (1) and indicates the relationship between the asymmetry measure extracted from cross-entropy analysis ($D(P_{Rt0} \parallel P_{Lt0})$) and the response that each limb presents to a thermal stimulus between two moments of time considered critical ($D(P_{t2} \parallel P_{t1})$). The values P_{Lt0} and P_{Rt0} correspond to the probability functions of the left and right legs in a basal state, respectively, while P_{t1} and P_{t2} correspond to the probability functions of the legs in the immediate instant after applying the thermal challenge, and a subsequent recovery moment after 15 s, respectively. The method for obtaining those measurements is described in refs [7,17].

$$ATR = \frac{\bar{D}(P_{t2} \parallel P_{t1})}{\bar{D}(P_{Rt0} \parallel P_{Lt0})} \tag{1}$$

Since the thermal evolution and the relative asymmetry are evaluated simultaneously, it strengthens the significance of the ATR-index as a parametric descriptor of the general behaviour of the temperature distribution in the lower extremities. According to the objectives of this work, we will have a series of thermal images for each subject at different times after applying an external stimulus. For this purpose, it is proposed to use the ATR-index as a function of time t_i according to Equation (2), where t_i represents the index of the thermal image in the temporal acquisition. This makes it possible to evaluate the asymmetry based on the metabolic evolution in the face of an induced thermal change.

$$ATR(t_i) = \frac{\bar{D}(P_{t2} \parallel P_{t1})}{\bar{D}(P_{Rti} \parallel P_{Lti})} \tag{2}$$

2. Methodology

2.1. Cohort selection

In accordance with the objectives of this study, it is necessary to establish two study groups with adequately differentiated clinical characteristics and supported by a complete clinical evaluation, including studies of biochemical parameters and a specialised medical evaluation. The cohort consisted of 54 adult subjects (40–75 years old), homogeneous in terms of socioeconomic status and geographical origin. The patient group consists of 36 subjects with a clinical diagnosis of DM2 with a progression of at least 5 years, whose medical evaluation reports varying levels of peripheral damage without presenting characteristic lesions related to DFD. The control group consists of 18 participants with a negative clinical diagnosis of DM2. The clinicodemographic data from the study cohorts can be reviewed in Table 1.

Table 1. Clinicodemographic data of the study cohorts, divided according to the study group and whose statistical dispersion is described according to the standard deviation (SD). BMI: Body Mass index; HbA1c: glycated haemoglobin; blood glucose level (BGL).

Group	Age (±SD) [years]	BMI (±SD) [kg/m^2]	BGL (±SD) [mg/dL]	HbA1c (±SD) [%]
Patients group	59.43(±9.36)	28.35(±3.64)	164.818(±72.58)	8.63(±2.5)
Female				
Male	57.76(±8.3)	27.88(±3.26)	159.53(±69.4)	8.29(±3.74)
Control group	48.33(±9.2)	27.67(±3.61)	91.6(±7.05)	5.58(±0.24)
Female				
Male	52.16(±5.11)	27.71(±3.84)	94.2(±6.67)	5.65(±0.35)

Following what was established by the clinical protocol (ID number DI/10/301/4/115) carried out at the General Hospital of Mexico (HGM of the Spanish Hospital General de México), all patients are adequately informed about the nature and purpose of the study. After that, they sign in accordance and give their consent for the use of their data. Both the treatment of the subjects and the consent to provide information were strictly carried out by the assigned clinical and medical staff of the HGM.

2.2. Acquisition of IR-images

To ensure high-quality infrared images (IRIs) in each acquisition session, it is necessary to minimise any source of thermal noise, so a suitable space has been created where humidity and temperature can be controlled. This requirement is to prevent and maintain the registry of abnormal changes in the images or environmental conditions due to affecting the IR-camera performance. For image acquisition, the FLIR-A320 infrared camera was used, which has a thermal resolution of 0.05° C. The dynamic range of temperatures in the IR-images goes from $T = 20°$ C to $T = 38°$ C. Adjustments were made to the following camera parameters based on both environmental variables and the radiation source. The thermal emissivity parameter was set at 0.95, while the relative humidity was below 60% and the room temperature remained at 20° C ±2° C according to the recommendations described in [2].

It should be noted that, as can be seen in Figure 1, the distance between the studied individuals and the infrared camera was kept fixed at 1 m, while the camera was positioned at a height of 40 cm from the ground, so that its axis of vision and the anteroposterior axis of the individual's body remained always parallel. Meanwhile, the apparent reflected temperature was modified for each acquisition according to the changes observed in the scene.

The region of interest (ROI) that the study focuses on corresponds to the one formed between the tibioperoneal trunk and the origin of the foot's dorsal artery, as it is a distinctive region that is frequently affected by both peripheral vascular disease and neurological damage associated with DFD. For each subject participating in this study protocol, an infrared image acquisition session was performed, from which two IR image sequences of the ROI of interest were obtained: one in the frontal view and one in the posterior view.

The first images of each sequence correspond to the baseline state and are detected at the time referred to as t_0. To acquire these first images, each subject must undergo a 15-minutes relaxation procedure during which each subject was instructed to discover the area of interest, avoiding crossing their legs and placing the soles of their feet on the ground. The following images are detected immediately after inducing thermal stress; this time is labelled as t_1. From then on, a new image is detected every 15 s, until $n = 16$ IR-images are obtained per view taken at instant of time t_n. Thermal stimulation was performed by simultaneously cooling both legs using commercial wet wipes.

Figure 1 graphically summarises the acquisition methodology described.

A fundamental feature of this methodology is the ability to achieve mild thermal stress through humidification of the skin, which causes limited vasoconstriction due to the simultaneous cooling of both lower extremities. To achieve this, two wet wipes that come into contact with the skin of the lower extremities are used simultaneously. The underlying hypothesis is that in any individual free from any condition related to metabolic syndrome, both limbs would recover a temperature distribution very similar to that of their basal state at a synchronised pace, while an individual with some evolution of metabolic syndrome would experience an asymmetric recovery due to the presence of different states of neuropathy or vasculopathy [31–33].

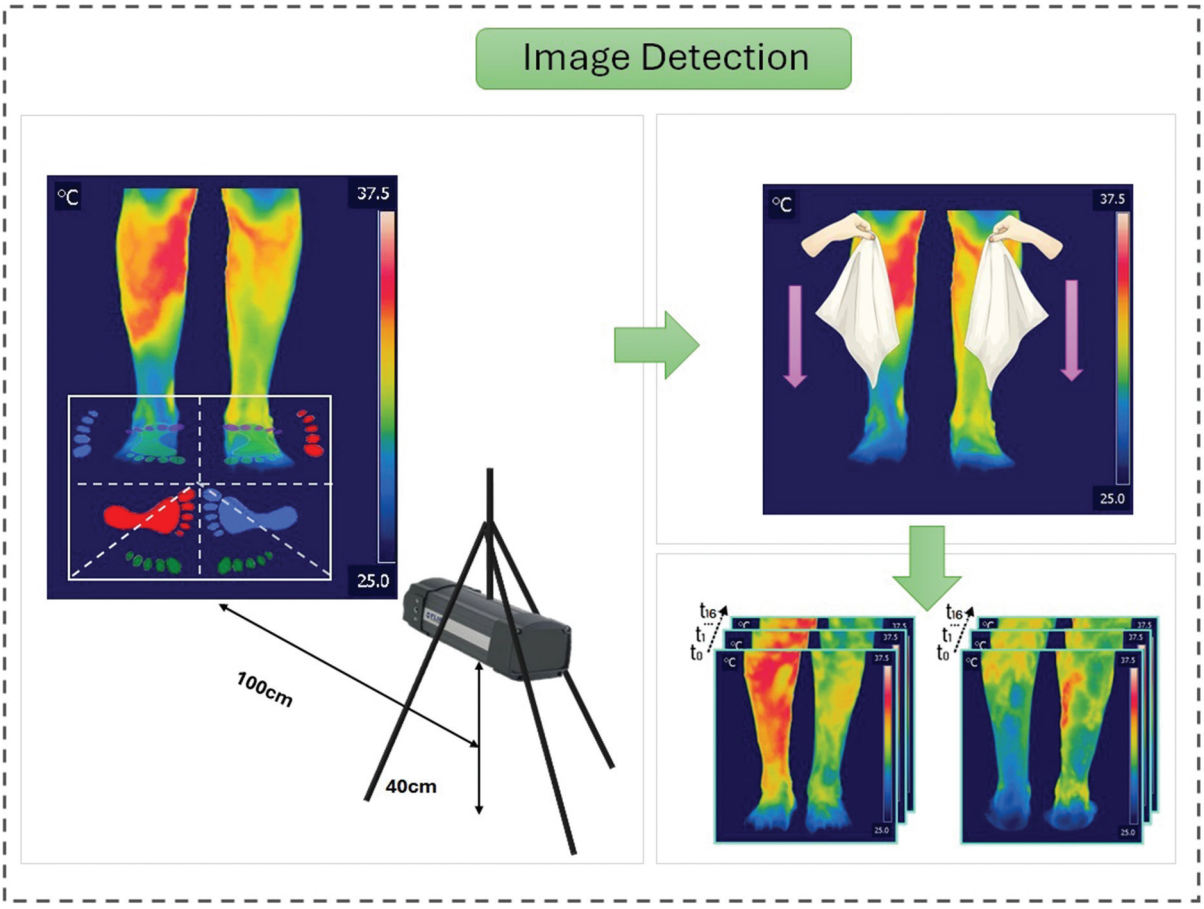

Figure 1. General diagram of the proposed method for detection of IRIs. We got two sequences of IRIs of the lower extremities of each subject in the study, one for the frontal view and the other for the posterior view.

For the current protocol, the number of images, and thus the corresponding time span, is good enough for describing the indices and the relationships emerging from thereafter; then, the current cut-off criteria can vary accordingly with the desired data refinement or any further requirement.

Additional details about the acquisition of IR-images have been previously reported in refs [6,17,23].

2.3. IR-images analysis

From the study of the IR-images of each participating subject, the radiometric information corresponding to each time t_n is extracted. The image segmentation procedure implemented in this study is based on a global intensity thresholding approach applied to normalised thermal images. Initially, each thermal image is converted into a greyscale representation and subsequently normalised to the range [0,1] using a linear scaling function. Segmentation is then performed by applying a predefined global threshold through a binarisation process. This operation yields a binary mask in which pixels with intensity values exceeding the threshold are classified as part of the ROI, whereas those below the threshold are assigned to the background. The resulting binary mask is used to isolate the ROI by selectively preserving the corresponding pixel intensities from the original thermal image while suppressing background contributions. Furthermore, the segmentation process is spatially limited to a predefined region specified by coordinate bounds, ensuring that the analysis is restricted to the anatomically and functionally relevant areas. This constraint improves the computational efficiency and the consistency of the segmentation process.

Once the ROI is segmented, this is divided into two regions: one contains the radiometric information of the left leg I_{Lt} and the other that of the right leg I_{Rt}. For each pair of images, a temporal index $ATR(t_i)$ is obtained, following Equation (2).

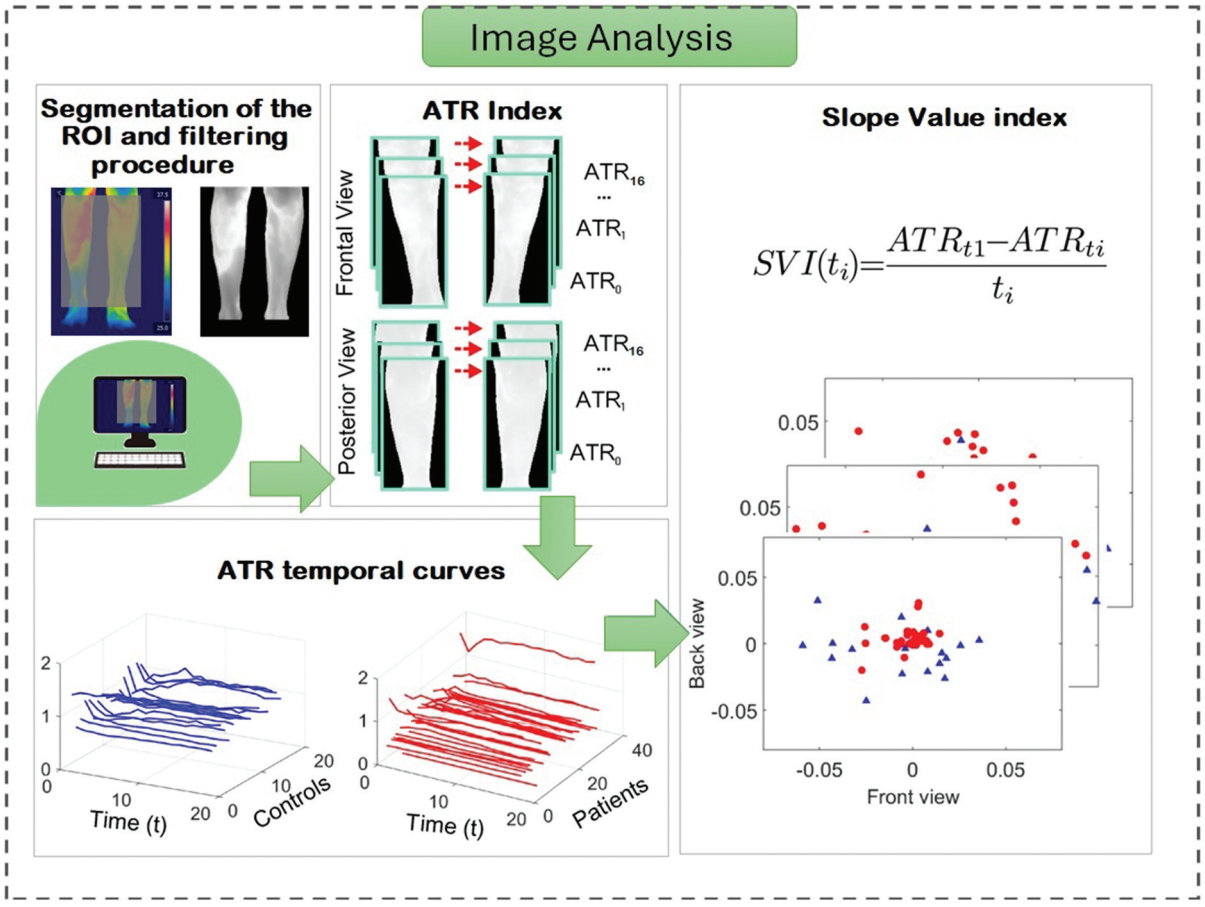

Figure 2. General diagram of the proposed method for analysis of IRIs. We got two sequences of IRIs of the lower extremities of each subject in the study, one for the frontal view and the other for the posterior view. The image analysis comprises several steps to get: (1) the ATR-index for each IRI, (2) the time curves using the ATR values, and (3) the distribution for the SVI (Slope Value Index).

By following the evolution of this index through a time-dependent curve, we can determine the metabolic response of each participating subject to a thermal stimulus over time. To visualise this response in relation to the baseline state, we propose a thermal response quantifier called the slope value index (SVI), which is defined as:

$$SVI_i \triangleq SVI(t_i) = \frac{ATR_0 - ATR_i}{t_i}. \tag{3}$$

Here, t_i represents the instant of image acquisition time. In turn, $ATR_0 \triangleq ATR_{t0}$ is the asymmetry index evaluated in the basal state; ATR_i is the value extracted from the IR images pictured at the corresponding time t_i. Here $i = 1,2,3,\ldots,n$.

Figure 2 graphically summarises the analysis methodology described.

3. Results and interpretation

The SVI distribution graph is described in terms of Equation (2) for each time (t_i), for both the front view (x-axis) and the back view (y-axis). An example of this is shown in Figure 3, which corresponds to the SVI distribution of patients and controls at time $t_8 = 105$ *s*.

For each instant of time (t_i), a threshold was determined by optimising the sensitivity and specificity values. These sensitivity and specificity values were always greater than 80%, suggesting confidence in the robustness of the SVI index at each instant of time in a temporal evaluation. The ROC space map of the SVI index for all evaluation times is shown in Figure 4.

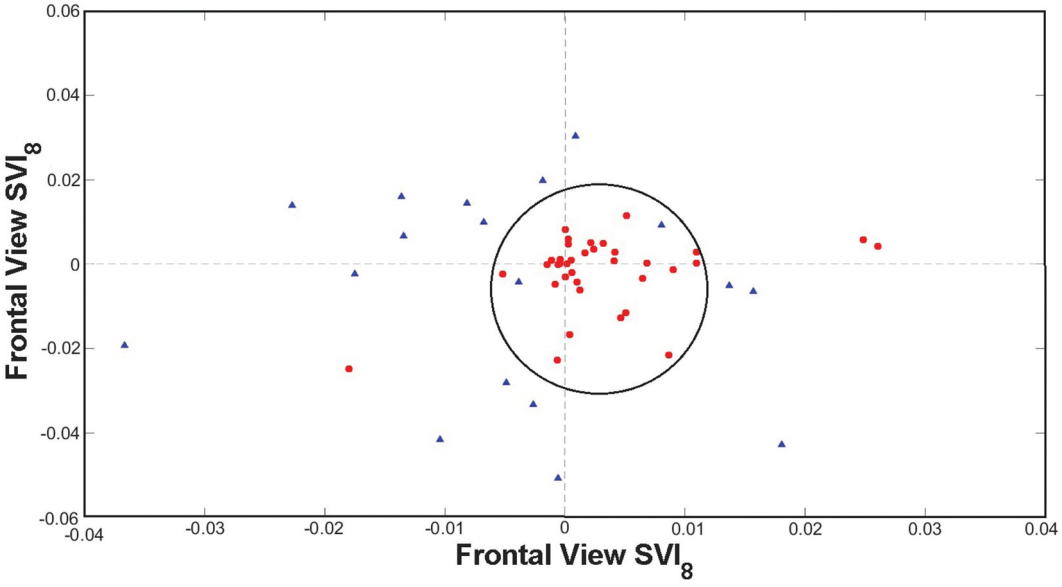

Figure 3. Example of distribution of the SVI index for $i = 8$, and thus corresponding to the label $t_8 = 105$ *s*. The triangle markers (▲) depict the corresponding control output; instead, the circle markers (•) refer to the patients. The x-axis relates to values extracted from the anterior view, whereas the y-axis is for those from the posterior view. This example is provided to display the maximum compactness of patient data, around the origin and highlighted with the drawn circle, and in contrast with the control group data; those are broadly scattered.

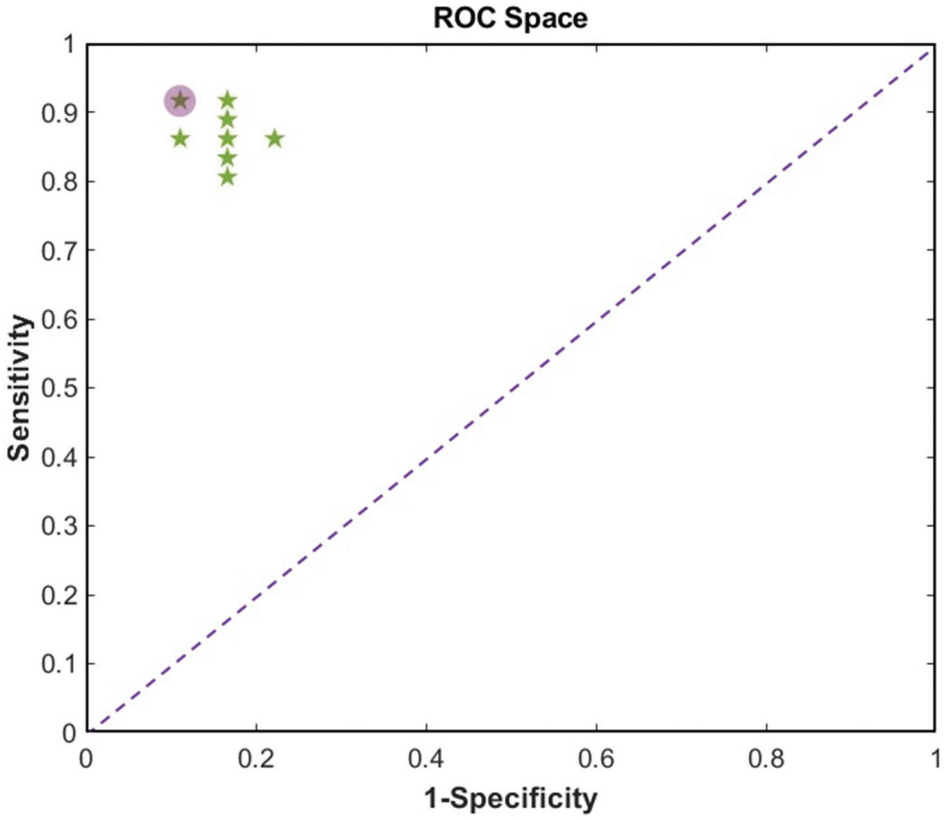

Figure 4. ROC space of the SVI index for all evaluation times t_i. The optimal cut-off value is indicated within a circle according to the Youden's index, which is detected at the times $t_8 = 105$ *s* and $t_9 = 120$ *s*. The ROC analysis yielded an area under the curve (AUC) of 0.95 (95% CI: 0.92–0.98).

Taking as a starting point the data in the ROC's representation space, when evaluating the SVI index at different times (t_i), we see that for all times there is a statistically significant classification between groups. However, according to the Youden's index, the optimal cut-off value occurs at $t_i = t_8$ and $t_i = t_9$, which corresponds to the time interval from 105 to 120 s after applying the thermal stimulus. For both cases, the sensitivity and specificity are 92% and 83%, respectively.

From the radiometric information content of each IR image, we can understand the general behaviour of each group in a temperature regulation process. This was carried out by estimating the average values of the SVI index for each instant of time (t_i) in both groups, to obtain the SVI_i of the frontal view (SVI_{Fti}) and the SVI_i for the posterior view (SVI_{Bti}). The results related to these indices show that there is a significant difference in the average behaviour of each group, as evidenced in Figure 5. It also shows that the response to external temperature stimulus is greater in the control group than in patients. This implies that subjects with DM2 exhibit poor performance in thermoregulation processes, which is consistent with the consensus [6,11,28,34,35].

Furthermore, Fig. 5 shows that in the control group the average temporal behaviour of the SVI curves for the anterior and posterior views presents similar characteristics, suggesting a corresponding linear relationship between the temporal performance of the limbs in both views with respect to the temperature regulation process. However, in the group of patients with DM2, uneven performance was observed between the curves of the anterior and posterior view, as a consequence of the metabolic imbalance that compromises performance in temperature regulation processes. In addition, symmetry is compromised, causing a clear variation in the thermal response between the left and right extremities.

From the distribution of the data presented in Figure 3, the tendency of the position of each group with respect to the origin of the coordinates becomes evident; the patient group tends to be located closer to the origin, unlike the control group. This behaviour suggests that metabolic performance is related to the position of the SVI index relative to the origin. From this inference, it is relevant to know the distance of each subject's

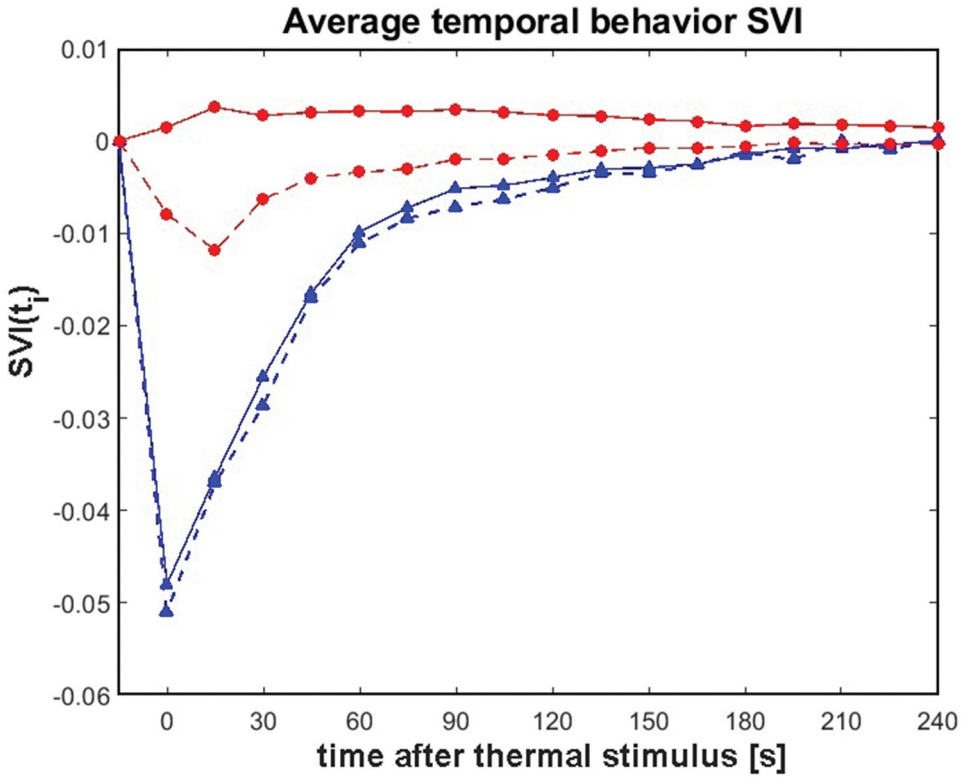

Figure 5. Average temporal behaviour between the group of patients and controls according to the SVI index. The triangle-marker lines correspond to controls (solid line relates to frontal view, dashed line for posterior view) and the circle-markers lines correspond to the behaviour of the patients (solid line for frontal view and dashed line for posterior view). The time span for recorded behaviour in all individuals is 225 seconds, being $t_1 = 0$ *s* the instant immediately after manual humectation.

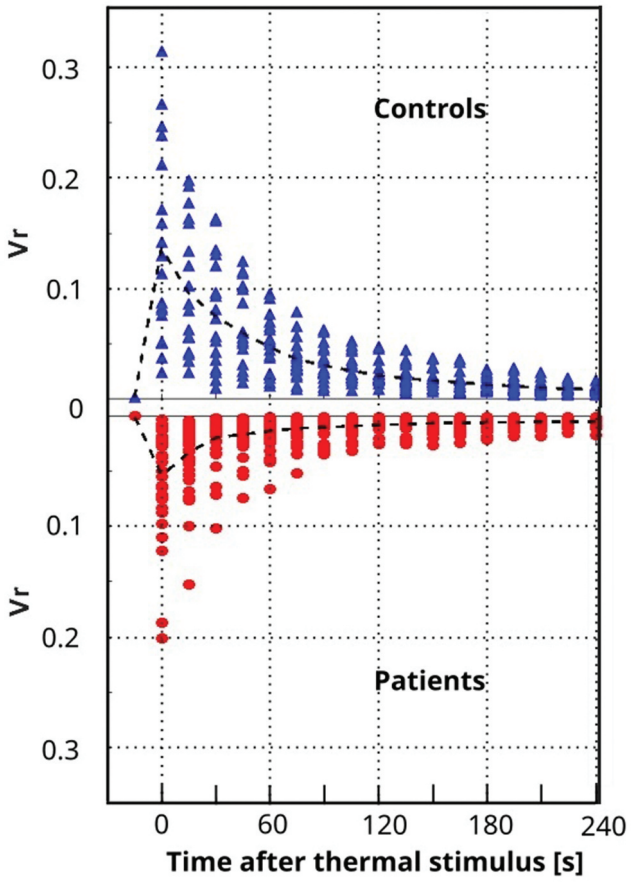

Figure 6. V_r distribution of the groups of patient and control subjects. The graph shows the time-dependent V_r distribution of each individual in the control (▲) and the patient (•) groups. The dashed lines depict the average value $\overline{V_{ri}}$, out of Eq. (4), for control subjects (▲), and patients (•). The mirror display is for didactic comparison of the V_r value between controls (upper-half) and patients (lower-half).

position relative to the origin in the SVI index representation diagram. Therefore, we introduce the parameter $V_{ri} \triangleq V_r(t_i) = \sqrt{SVI_{Fti}^2 + SVI_{Bti}^2}$, calculated for each time t_i. This new parameter allows us to construct a curve that represents the temporal behaviour of each subject for both study groups, as shown in Figure 6. The statistical average of the temporal performance of each group is shown in dashed lines and represented as

$$\overline{V_{ri}} = \frac{1}{N}\sum_{j=1}^{N} V_{ri_j}; \tag{4}$$

where N is the total number of subjects in each group. Here, for each V_{ri} point in time, we calculate the average over all the subjects of each group, and then we plot all the averages on time.

The parameter $\overline{V_{ri}}$ was computed for both groups, for each time, and represented in Fig. 6 by the black dotted line in both cases.

Since we deal with the average values for $\overline{V_{ri}}$, it would be expected that by including new patient and control data in the data analysis, the new values of $\overline{V_{ri}}$ would only shift the relative values around the current ones, providing greater precision to the relative positions. A much longer and more ambitious task is to include patients diagnosed with DM2 who are following a specific medical treatment for the disease; it is expected that these will be within the upper limits of the group.

The V_{ri} index has a particular significance. It opens up conditions for standalone quantitative scaling of the IR-image-related asymmetry. Since $V_{ri}^2 = SVI_{Fti}^2 + SVI_{Bti}^2$, one expect that given any two different values of the SVI-index in the anterior view and the SVI-index in the posterior view, one can construct parametric pairs of entries, that is, $\left[(SVI_{Fti}, SVI_{Bti}), (SVI_{Ftj}, SVI_{Btj})\right]$ with $i \neq j$. Nevertheless, as the anterior and posterior views are spatially independent, although they belong to the same body, this condition alone does not guarantee that these

indices, associated with each image view, would produce information such that what is obtained from one view interleaves in a linear manner with the complementary other view. This is an important feature from the perspective of disclosing the true extent to which the quantitative nature of the asymmetry and the stand-alone value of the information extracted within such scope. Since one can get parametric pairs, in an analogous sense as in a vector construction, then it is immediate to enquire if the Schwartz inequality is truly satisfied. That is, to verify whether the inequality, $|SVI_{Fti} \cdot SVI_{Ftj} + SVI_{Bti} \cdot SVI_{Btj}|^2 \leq |SVI_{Fti}^2 + SVI_{Bti}^2 + SVI_{Ftj}^2 + SVI_{Btj}^2|$, is fulfiled.

This inequality implies that, statistically, the SVI-indices for the frontal and posterior views keep a linear relationship at each instant of time, provided that the associated images are acquired under the noted conditions. This result not only corroborates the assumption that there should be a correspondence in the thermal performance of both views of the lower limbs due to the linear relationship between the indices, but also implies that the values of the V_{ri} are well defined and bounded. This is a rather fundamental feature from the perspective that no matter the data distribution, these have to be on a quantifiable and bounded scale. The extent of the number of consequences requires a dedicated framework where the already known conditions are well defined, and thus discloses further details of the resulting framework. Clearly, such analysis is away from the current scope and is likely to be covered in later contributions.

4. Discussion and conclusions

The SVI index makes it possible to identify the metabolic response in both groups at different points in time. As seen in Figure 3, the patient group shows less dispersion in the distribution of SVI index values than the control group. This indicates a probable homoeostatic imbalance in the patient group, because DM2 induces deterioration in various mechanisms necessary for temperature regulation [6,27,28,36]. A summary of the metabolic response of both groups over time can be seen in the graph in Figure 5, where the differences in the metabolic response presented by the group of patients with respect to the control group become evident. As can be seen, the control group showed a greater response to a vasoconstriction challenge and a more symmetrical evolution during the temperature regulation process.

In order to know how the metabolic response is individually, the parameter V_{ri} is proposed, defined as the distance from the SVI index to the origin of the coordinate space formed by the front and back views. According to the results obtained from the temporal analysis developed with the parameter V_{ri} in all the individuals participating in the study, it is evident that there is a statistically significant difference between both groups according to the Mann-Whitney U test, with a statistical significance of $p < 0.0001$ for all the characteristic parameters of both population groups (patients and controls). Due to the alterations that the presence of diabetes causes in the temperature regulation processes, the observed differences can be associated with the presence of type 2 diabetes.

This last result demonstrates the ability of the indices proposed in this contribution to identify deficiencies in the metabolic performance of individuals with DM2 in the process of induced temperature regulation, providing a well-defined and limited measure. To determine the association between this measure given by the indices and clinical markers for the evaluation of glycaemic controls such as glucose and HbA1c, it is necessary to establish a statistical correlation. Thus, using the parameter V_{ri} this correlation was corroborated. The statistical results of these correlations indicate that V_{ri} has a significant correlation with glucose ($p < 0.01$) and HbA1c ($p < 0.001$).

In conclusion, the indices proposed in this study are able to quantify the thermal response to a thermal challenge in the lower extremities, providing information on peripheral impairment in patients diagnosed with DM2. Another important feature is that the indices also display robust properties that allow for self-referential analysis of thermal patterns. This self-referential analysis, based on the statistical analysis of radiometric information through the $SV\ I$ and V_r, which in a more fundamental way are based on cross-entropy analysis, provides a more robust tool than analyses based on direct temperature measurements, such as the average, since it allows extracting additional information from the spatial and spectral distribution of thermal patterns potentially associated with the aetiologies of DM2. It is worth noting that this self-referential approach is based on the underlying hypothesis that certain parameters external to the analysed system, in this case the subjects' lower limbs, do not influence the final value of the proposed indices. This would increase their value by making them more robust, even under less controlled environmental

conditions, such as those commonly encountered in clinical practice. However, this hypothesis is currently under investigation.

A medium-term expectation is to expand the available data with a much larger cohort to refine the scale of these indices as well as their general trend in terms of the temporal evolution of asymmetry. It is expected that by including a larger sample, the underlying physiological trends captured by the proposed quantitative indices will remain consistent. The linear property, as described, requires further consideration if a complete analytical framework is to be obtained. However, the corresponding advance in that stage of the theoretical model requires further research, which is far from the current scope.

The long-term possibility with this methodology is to achieve a rating scale that allows inferring manifestations of asymmetry in patients in not so advanced stages of diabetes mellitus, in such a way that disease states that lead to amputations can be prevented, so that the extenuating cost for any medical system and for the patient can be reduced.

Acknowledgements

Rosalinda Ortiz-Sosa acknowledges the support of the postdoctoral position at ICAT-UNAM, granted by the Consejo de Ciencia, Tecnología e Innovación de Hidalgo (CITNOVA). C. GarcíaSegundo gratefully acknowledges the PASPA-DGAPA programme at UNAM for the sabbatical support as a visiting researcher at the Institute of Biological and Medical Imaging, Helmholtz Zentrum, München, Germany. He also gratefully acknowledged Prof. Frank Filbir for his support as host during the stay. All UNAM-related authors gratefully acknowledge the financial support through the PAPIIT-UNAM IG100821.

Author contributions

CRediT: **Rosalinda Ortiz-Sosa:** Conceptualization, Data curation, Formal analysis, Investigation, Methodology, Writing – original draft; **Edgar I. Fuentes-Oliver:** Conceptualization, Data curation, Formal analysis, Investigation, Writing – review & editing; **Raúl Serrano-Loyola:** Supervision, Validation; **Rebeca Solalinde-Vargas:** Validation; **Crescencio García-Segundo:** Funding acquisition, Investigation, Methodology, Writing – review & editing.

Disclosure statement

No potential conflict of interest was reported by the author(s).

Funding

This work was supported by the Universidad Nacional Autónoma de México under Grant [PAPIIT-UNAM IG100821].

ORCID

Rosalinda Ortiz-Sosa http://orcid.org/0000-0002-8416-3258
Crescencio García-Segundo http://orcid.org/0000-0002-7450-0935

Data availability statement

The data are available upon request of the corresponding author.

References

[1] Hall JE, Guyton AC. Textbook of medical physiology. Philadelphia: Saunders Elsevier; 2011.
[2] Ring E, Ammer K. The technique of infrared imaging in medicine. Thermology Int. 2000;10(1):7–14.
[3] Johnson JM, Minson CT, Kellogg DL. Cutaneous vasodilator and vasoconstrictor mechanisms in temperature regulation. Compr Physiol. 2014;4(1):33–89. doi: 10.1002/j.2040-4603.2014.tb00541.x
[4] Ammer K, Melnizky P, Rathkolb O, et al. Thermal imaging of skin changes on the feet of type II diabetics. In: Conference Proceedings of the 23rd Annual International Conference of the IEEE Engineering in Medicine and Biology Society. IEEE; 2001. Vol. 3. p. 2870–2872. doi: 10.1109/IEMBS.2001.1017387

[5] Johnson JM, Minson CT, Kellogg DL. Thermal symmetry of the upper and lower extremities in healthy subjects. Thermology Int. 2012;22:53–60.
[6] Fuentes-Oliver EI, García-Segundo C, Solalinde-Vargas R, et al. Anomalous contra-lateral radiometric asymmetry in the diabetic patient. Biomed Phys Eng Express. 2019;5(6):1–13. doi: 10.1088/2057-1976/ab49f5
[7] Ortiz-Sosa R, Fuentes-Oliver EI, García-Segundo C, et al. On the stability of asymmetry of thermal emission in diabetic foot disease. In: AIP Conference Proceedings. Vol. 2090. AIP Conference Proceedings; 2019. p. 050010. doi: 10.1063/5.0051109
[8] WHO. Global report on diabetes. World Health Organization. 2016. Available from: http://www.who.int/diabetes/global-report/en/
[9] IDF. Diabetes atlas. 11th ed. International Diabetes Federation; 2025. Available from: https://diabetesatlas.org/resources/idf-diabetes-atlas-2025/
[10] Diakides M, Bj D, Peterson DR. Medical infrared imaging: principles and practices. Boca Raton: CRC Press; 2013.
[11] Liu C, van der Heijden F, Klein ME, et al. Infrared dermal thermography on diabetic feet soles to predict ulcerations: a case study. In: Advanced Biomedical and Clinical Diagnostic Systems XI. Proceedings; 2013. p. 85720N–185720N8. doi: 10.1117/12.2001807
[12] Macdonald A, Petrova N, Ainarkar S, et al. Thermal symmetry of healthy feet: a precursor to a thermal study of diabetic feet prior to skin breakdown. Physiol Meas. 2017;38(1):33–44. doi: 10.1088/1361-6579/38/1/33
[13] Sheen YJ, Sheu WH, Wang HC, et al. Assessment of diabetic small-fiber neuropathy by using short-wave infrared hyperspectral imaging. J Biophotonics. 2022;15(2):e202100220. doi: 10.1002/jbio.202100220
[14] Cao Z, Zeng Z, Xie J, et al. Diabetic plantar foot segmentation in active thermography using a two-stage adaptive gamma transform and a deep neural network. Sensors. 2023;23(20):8511. doi: 10.3390/s23208511
[15] Godavarty A, Leiva K, Amadi N, et al. Diabetic foot ulcer imaging: an overview and future directions. J Diabetes Sci Technol. 2023;17(6):1662–1675. doi: 10.1177/19322968231187660
[16] Faus CM, Izquierdo-Renau M, Julian-Rochina I, et al. Update on the use of infrared thermography in the early detection of diabetic foot complications: a bibliographic review. Sensors. 2023;24(1):252. doi: 10.3390/s24010252
[17] Ortiz-Sosa R, Fuentes-Oliver EI, García-Segundo C, et al. Analysis of the density and distribution of entropy in biomedical infrared imaging for diabetes mellitus type II. Biomed Phys Eng Express. 2021;7(4):1–9.
[18] Avila-Cabrera D, Bayareh-Mancilla R, Vera-Hernandez A, et al. Clinical and thermographic database of patients with diabetes mellitus with perspective for quantitative studies. In: CCE 2022 – 2022 19th International Conference on Electrical Engineering, Computing Science and Automatic Control; 2022. doi: 10.1109/CCE56709.2022.9975973
[19] Carbonell L, Priego-Quesada JI, Retorta P, et al. Thermographic quantitative variables for diabetic foot assessment: preliminary results. Comput Methods Biomech Biomed Eng: Imag Visual. 2019;7(5–6):660–666. doi: 10.1080/21681163.2018.1542349
[20] Barriga ES, Chekh V, Carranza C, et al. Computational basis for risk stratification of peripheral neuropathy from thermal imaging. In: Proceedings of the Annual International Conference of the IEEE Engineering in Medicine and Biology Society. EMBS; 2012. p. 1486–1489. doi: 10.1109/EMBC.2012.6346222
[21] Loza-González VM, Martínez-Jiménez MA, Novoa-Moreno AL, et al. Diabetic foot ulcer healing with polylactic acid membrane assessed by thermographic imaging: a case report. Front Med (Lausanne). 2025;12:12. doi: 10.3389/fmed.2025.1568144
[22] Mrowiec A, Kasprzyk-Kucewicz T, Wziątek-Kuczmik D, et al. Use of thermal imaging in the detection of the diabetic foot- review. Rev Endocr Metab Disord. 2026;27(1):17–40. doi: 10.1007/s11154-025-09999-w
[23] Fuentes-Oliver EI, Ortiz-Sosa R, García-Segundo C, et al. Quantitative interpretation of infrared images of lower limbs in individuals with and without type 2 diabetes mellitus. Skin Res Technol. 2024;30(9):e70039. doi: 10.1111/srt.70039
[24] Barnes RB. Diagnostic thermography. Appl Opt. 1968;7(9):1673–1685. doi: 10.1364/AO.7.001673
[25] Jones BF. A reappraisal of the use of infrared thermal image analysis in medicine. IEEE Trans Med Imag. 1998;17(6):1019–1027. doi: 10.1109/42.746635
[26] Liu C, Netten JJ, Baal JG, et al. Automatic detection of diabetic foot complications with infrared thermography by asymmetric analysis. J Biomed Opt. 2015;20(2):026003.
[27] Bharara M, Viswanathan V, Cobb JE. Cold immersion recovery responses in the diabetic foot with neuropathy. Int Wound J. 2008;5(4):562–569. doi: 10.1111/j.1742-481X.2008.00454.x
[28] Balbinot LF, Canani LH, Robinson CC, et al. Plantar thermography is useful in the early diagnosis of diabetic neuropathy. Clinics. 2012;67(12):1419–1425. doi: 10.6061/clinics/2012(12)12
[29] Soliz P, Agurto C, Edwards A, et al. Detection of diabetic peripheral neuropathy using spatial-temporal analysis in infrared videos. In: 2016 50th Asilomar Conference on Signals, Systems and Computers; Boston (USA). IEEE; 2016. p. 263–267.
[30] Fuentes-Oliver EI, García-Segundo C, Serrano-Loyola R, et al. Quantification of thermal asymmetry in diabetic foot disease. In: AIP Conference Proceedings. Vol. 2090. AIP Conference Proceedings; 2019. p. 040002. doi: 10.1063/1.5095905
[31] Chandrashekar A, Gasparis A, Labropoulos N. Lack of symmetry in the major lower limb veins. J Vasc Surg: Venous Lymphatic Disord. 2017;5(3):346–352. doi: 10.1016/j.jvsv.2016.11.010
[32] Mayrovitz HN, Larsen PB. Pulsatile blood flow asymmetry in paired human legs. Clin Physiol. 1996;16(3):495–505. doi: 10.1111/j.1475-097X.1996.tb01015.x

[33] Crivellato E, Ribatti D. Body symmetry and asymmetry in early Greek anatomical reasoning. Clin Anat. 2008;21 (4):279–282. doi: 10.1002/ca.20626
[34] Bharara M, Viswanathan V, Cobb JE. Warm immersion recovery test in assessment of diabetic neuropathy - a proof of concept study. Int Wound J. 2008;5(4):570–576. doi: 10.1111/j.1742-481X.2008.00455.x
[35] Bagavathiappan S, Philip J, Jayakumar T, et al. Correlation between plantar foot temperature and diabetic neuropathy: a case study by using an infrared thermal imaging technique. J Diabetes Sci Technol. 2010;4(6):1386–1392.
[36] Agurto CSB, Burge M, Soliz P. Characterization of diabetic peripheral neuropathy in infrared video sequences using independent component analysis. In: 2015 IEEE International Workshop on Machine Learning for Signal Processing (MLSP); Boston (USA). IEEE; 2015. p. 1–6.